

High-Efficiency Synchronous Motors with Permanent Magnets

Jakub BERNATT^{1*} and Zbigniew SZKUDLAREK²

Authors' affiliations and addresses:

¹ KOMAG Institute of Mining Technology
Pszczynska Street 37, 44-101 Gliwice, Poland
e-mail: jbernatt@komag.eu

² KOMAG Institute of Mining Technology
Pszczynska Street 37, 44-101 Gliwice, Poland
e-mail: zszkudlarek@komag.eu

*Correspondence:

Jakub Bernatt, KOMAG Institute of Mining
Technology
Pszczynska Street 37, 44-101 Gliwice, Poland
e-mail: jbernatt@komag.eu

How to cite this article:

Bernatt J. and Szkudlarek Z. (2024). High-Efficiency Synchronous Motors with Permanent Magnets. *Acta Montanica Slovaca*, Volume 29 (4), 908-919

DOI:

<https://doi.org/10.46544/AMS.v29i4.10>

Abstract

The paper deals with highly efficient Permanent Magnet Synchronous Motors (PMSM) and Line Start Permanent Magnet Motors (LSPMM). LSPMM are well recognized and used, also in the heavy industry in the drives which do not need a change of the rotation speed, but they can not drive the machines requiring high starting torque or machines with big inertia torque (for example, mills or belt conveyors while fully loaded during start-up). The novel design of LSPMM with winding in the rotor was developed, described, manufactured and tested. LSPMM with winding in the rotor (LSPMMwWR) do not need frequency inverters for start-up and operation, and that kind of motor can be used for driving machines with big inertia torque or machines requiring high and long-lasting starting torque. The advantage of LSPMMwWR over LSPMM is characterized mainly by minimizing thermal losses in the rotor, which do not cause thermal overheating of permanent magnets, and also by higher starting torque. The experimental model of the LSPMMwWR was manufactured and tested, and the results are presented in the paper. Additionally, the paper shows an example of the use of PMSM in suspended trains for underground applications in coal mines. The train and the motors are supplied from lithium-ion batteries designed and tested for the explosion-risk areas.

Keywords

Permanent Magnet Synchronous Motor (PMSM), starting process, Line Start Permanent Magnet Motor (LSPMM), slip-ring motor



© 2024 by the authors. Submitted for possible open access publication under the terms and conditions of the Creative Commons Attribution (CC BY) license (<http://creativecommons.org/licenses/by/4.0/>).

Introduction

Synchronous motors, either electromagnetically or permanently magnetized, find widespread application in driving dewatering pumps and ventilation fans in mine ventilation systems, as well as in the milling processes of ore enrichment plants in the copper industry and in power units of tyre and rail vehicles operated in underground mining. Given that ventilation and dewatering systems collectively consume approximately 40% of a mine's total electrical energy, the deployment of energy-efficient drives in these applications is paramount. However, the starting behaviour of synchronous motors, from standstill to synchronous speed, presents a significant engineering challenge, which this article aims to address.

Slip-ring induction motors (SRIMs) are well-known synchronous motors. These are induction motors with slip rings. The motors are started using starting resistors connected to the rotor winding circuit through slip rings and brushes. The starting current usually does not exceed twice the rated current value, while the starting torque is significantly higher than the rated torque. After starting, the rotor winding is supplied with direct current, and the motor synchronizes itself automatically, and after synchronization, it operates as a synchronous motor. Compared to slip-ring induction motors performing the same task, the advantage of these motors is higher efficiency and a higher power factor $\cos \phi$. These motors are used in high-power drives and are directly supplied from the power grid with a voltage of 6 kV or 10 kV. The disadvantage of this solution is the excitation system, power losses in the excitation circuit, which reduce the efficiency of the drive system. Additionally, the slip rings require periodic inspection and cleaning, and the brushes wear out and need to be replaced. On the other hand, permanent magnet synchronous motors (PMSM) in standard designs are supplied from inverters controlled by the rotor position angle relative to the stator winding phase axes, so-called power electronic commutators. For high-power motors, building power electronic commutators for high voltage is costly. However, permanent magnet synchronous motors driving working machines operating at a constant rotational speed can be supplied directly from the power grid with a voltage of 6 kV or 10 kV (Line Start Permanent Magnet Synchronous Motor). The main problem with such solutions is motor starting.

Rotors' design

From the literature (Gwoździewicz, Zawilak, 2013; Zawilak, 2014, 2015; Bao, Mehmood and Feng, 2012), a synchronous motor whose rotor has both permanent magnets and a squirrel cage winding, is known. The permanent magnets are placed in slots in the middle of the rotor yoke, and the squirrel cage winding consists of non-insulated copper bars placed in slots on the outer circumference of the rotor and shorted by end rings.

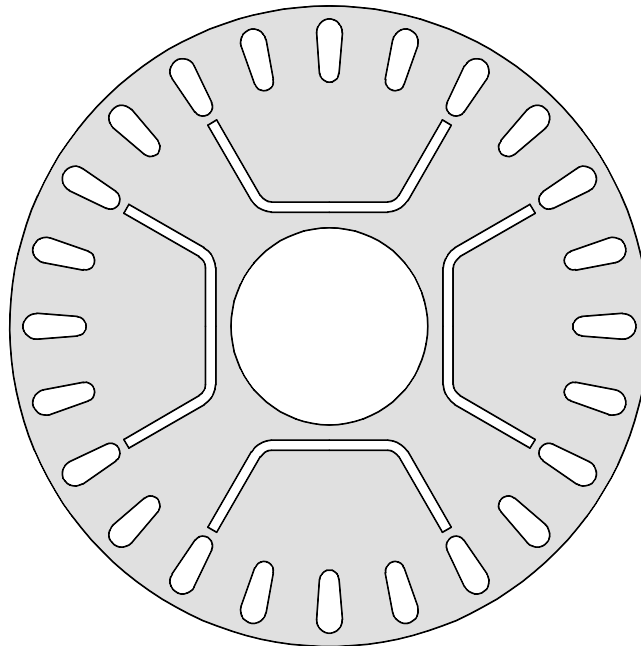


Fig. 1. Lamination of rotor's core with slots for squirrel cage and permanent magnets

Fig. 1 shows an example of the shape of a rotor lamination with visible slots for permanent magnets and slots for the squirrel cage winding. The squirrel cage winding is used to start the motor asynchronously. When the rotor reaches a subsynchronous speed during starting, the magnetic flux of the permanent magnets automatically

synchronizes it, and the motor operates as a synchronous motor. However, during starting, the asynchronous electromagnetic torque generated by the squirrel cage winding, at speeds from zero to about half the rated speed ($0 \leq n \approx 0.5 n_N$), is significantly smaller than the rated torque of the motor, while the starting current is 5 to 7 times higher than the rated current. In addition, after applying the voltage during the first half-cycle, there is a surge current and a surge torque. The starting current in the stator winding interacts with the flux of the permanent magnets and excites variable components of torque and force, which generate vibrations and noise. In addition, heat is generated in the squirrel cage, approximately equal to the kinetic energy of all rotating masses coupled to the motor shaft. This heat causes an increase in the temperature of the squirrel cage and threatens the thermal demagnetization of the permanent magnets.

Motors with a squirrel cage starting winding and permanent magnets in the rotor can be used to drive mechanical devices and working machines with short start-up times, for instance, to drive pumps where the moment of inertia is small and the load torque is a quadratic function of rotational speed. However, many working machines have a high starting torque, often greater than the rated torque of the motor, for instance, mine ventilation fans, gas exhaust fans in power plants, clogged coal mills in power plants in copper ore enrichment plants and others (Korski et al., 2023; Bołoz, 2024). Mechanical devices and working machines with a high moment of inertia are characterized by long start-up times. The use of a motor with permanent magnets and a squirrel cage starting winding is not advantageous for driving the mentioned mechanical devices and working machines. The starting of the motor can be significantly softened, and the starting time can be extended by making a slip-ring starting winding (Bernatt et al., 2017). The winding is three-phase, made of insulated copper wire, and is connected in a star or delta. The ends of the phases are connected to three slip rings located on the rotor shaft. The mutual arrangement of the permanent magnets and the winding on the rotor:

- the permanent magnets are placed in slots in the rotor yoke, and the winding is placed in slots on the rotor circumference - Fig. 2,
- the permanent magnets are placed on the circumference of the rotor yoke, and the winding is placed in slots under the permanent magnets - Fig. 3.

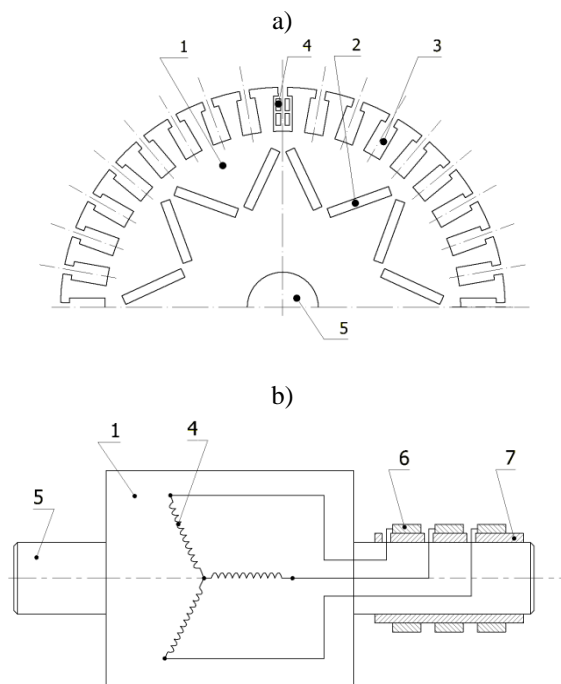


Fig. 2. Rotor of a synchronous motor with permanent magnets: a) cross-section of the rotor, b) star-connected winding with phase ends connected to slip rings

In Fig. 2, the rotor consists of a laminated stack forming a yoke 1, mounted on a shaft 5. Inside the yoke 1, there are slots 2, usually rectangular, in which permanent magnets are placed. The slots for the permanent magnets may also have a different shape. On the outer circumference of the yoke 1, in slots 3, a winding 4 is placed. The winding 4 of the rotor is three-phase, made of insulated copper wire and is connected in a star or delta. The ends of the phases of winding 4 are connected to three slip rings 6 located on an insulating sleeve 7, which is mounted on shaft 5 of the rotor. The conductors connecting the ends of winding 4 to slip rings 6 can be routed along the surface of shaft 5 or inside the hollow shaft 5. In a motor assembled on slip rings 6, there are brushes. The brushes, preferably copper-graphite, are placed in a brushgear. The brushgear, together with the brush lifting system, is usually mounted on the motor's bearing shield.

The electric motor with a rotor designed as described above can be used to drive working machines with high starting torque and mechanical devices with long start-up times. The motor is started using starting resistors. The starting current and starting torque can be controlled by the value of the connected resistance and its gradation as a function of rotational speed. More heat is generated in the starting resistors during motor starting than in the rotor winding. There is no risk of overheating the permanent magnets. After starting, the motor synchronizes itself and operates as a synchronous motor excited by the magnetic field of the permanent magnets. After motor synchronization, the brushes on the slip rings 6 are lifted to prevent wear and reduce friction losses. This type of motor can be used for any type of drive.

During synchronous operation, the motors are powered directly from the power grid, for instance, 6 kV or 10 kV, and have higher energy efficiency and power factor $\cos \varphi \approx 1$ compared to induction motors performing the same task. The permanent magnets placed inside the rotor yoke have greater dispersion and a smaller magnetic flux in the air gap, which affects the torque overload capability. With large disturbances of the load torque or voltage drops, the motor may fall out of synchronism.

Fig. 3 shows a rotor with permanent magnets mounted on the outer circumference. In this solution, the problem is the location of the starting winding, which must be placed in the rotor slots. The slots can be placed between the permanent magnets or under the permanent magnets. The winding should be m-phase-symmetrical. The number of phases can be reduced to $m = 2$ – Fig. 3a. In the slots between the magnets, only one phase can be placed. It is possible to make a symmetrical winding placed in the slots on the outer circumference by dividing the arc of the permanent magnet of each pole into two parts and placing a second slot between them - Fig. 3b. With this arrangement of slots, a symmetrical phase winding is feasible. If calculations show such a need, additional slots can be placed under the permanent magnets - Fig. 3c. The ends of the winding are connected to three slip rings mounted on an insulating sleeve located on the motor shaft.

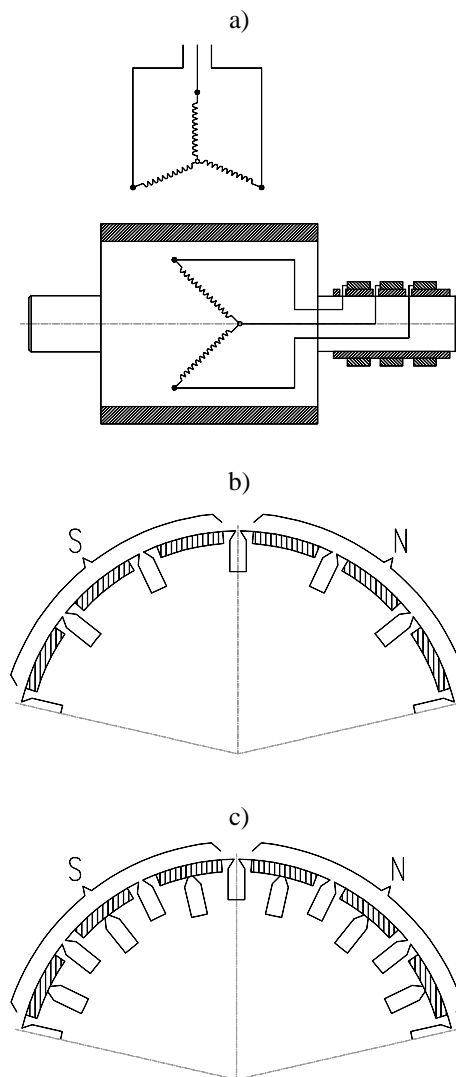


Fig. 3. Synchronous motor with permanent magnets and a starting winding:
 a) winding diagram, b) slot arrangement between permanent magnets, c) additional slots under permanent magnets

A synchronous motor with permanent magnets located on the outer circumference of the rotor has a small air gap between the stator and the rotor. The air gap is determined solely by mechanical considerations. The magnets have minimal leakage flux and maximum main flux. During starting, the asynchronous torque is determined by the stator winding and the rotor winding currents. By using a slip-ring winding, the starting current can be controlled by resistors connected to the rotor winding circuit through slip rings. The asynchronous characteristic as a function of rotational speed is shaped by the resistance of the resistors, which can be varied so that the starting current does not exceed the permissible value at a given motor connection point to the power grid. At subsynchronous speed, self-synchronization of the rotor occurs due to the magnetic flux of the permanent magnets. After synchronization, the motor operates as a synchronous motor. The rotor winding is shorted and serves as a damper winding to dampen rotor oscillations. During synchronous operation, the motor's maximum torque is proportional to the excitation flux. The excitation flux, with magnets on the rotor surface and a small air gap, is greater than that of magnets placed in the yoke. During synchronous motor operation, the power factor $\cos \varphi$ is more favourable, and the torque overload capability is higher. During starting, the currents in the stator and rotor windings, compared to the squirrel cage winding, are significantly smaller. The start-up is smoother. Such a start-up can be used for motors driving working machines with a long start-up time.

Model of the motor with permanent magnets and starting winding

The model motor was built based on the SUDfL-100B slip-ring induction motor (Glinka T., Bernatt J, 2017). The stator of the electric motor, i.e., the yoke and winding, is identical to that of the induction motor. The rotor lamination profile was changed. On the outer circumference, there are slots where the starting winding is located. Inside the yoke are rectangular slots in which permanent magnets with dimensions $109 \times 22 \times 4$ are placed - Fig. 4. The rotor winding is a slip-ring, as the aim was to measure the current during start-up. However, calculations and measurements were carried out with the rotor winding shorted.

Calculations of the magnetic induction distribution in the magnetic circuit of the machine, excited by permanent magnets, were carried out using the 2D FEM method in the Ansoft Maxwell 2D program.

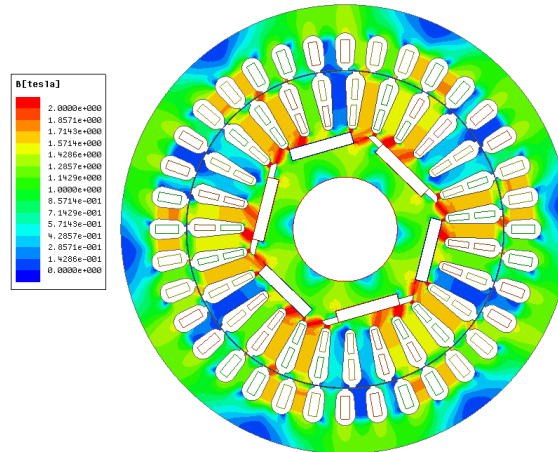


Fig. 4. Magnetic field distribution in a motor excited by permanent magnets

Calculated and rated parameters of the motor for synchronous operation: $P_N = 1.7$ kW; $U_N = 3 \times 400$ V; $I_N = 3.3$ A; $f_1 = 50$ Hz; $n_N = 1000$ rpm, $T_N = 16.2$ Nm; $T_{max} = 1.85 \times T_N$; $\cos \varphi = 0.9$; $\eta = 83\%$. Permanent magnets: N42UH; $B_r = 1.3 \times T_N$; $H_{CB} = 848$ kA/m; $\mu_r = 1.085$.

Calculations of the starting and synchronous characteristics were performed using the field-circuit method. The magnetic flux excited by the permanent magnets during starting induces a rotational voltage in the stator winding with an electrical frequency of rotation:

$$f_2 = \frac{n}{60} \times p \tag{1}$$

In the winding, a current flows that has two components: a network component I_1 with a frequency of $f_1 = 50$ Hz and a component I_2 with a frequency of f_2 . The current component I_1 generates an asynchronous torque T_a , determining the motor start-up, and the current component I_2 generates a synchronous torque T_{PM} , which, with changing rotational speed, is a variable torque that disturbs the start-up process. For the model motor, the average asynchronous torque characteristics T_a , T_{PM} and T_{wyp} were calculated with the rotor winding shorted. The resulting (average) starting torque of the model motor is calculated as the sum of the torques $T_{wyp} = T_a + T_{PM}$. Calculations

were performed at the Institute of Drives and Electric Machines KOMEL using the Ansoft Maxwell 2D program. The calculated average starting torque characteristics are presented in Fig. 5.

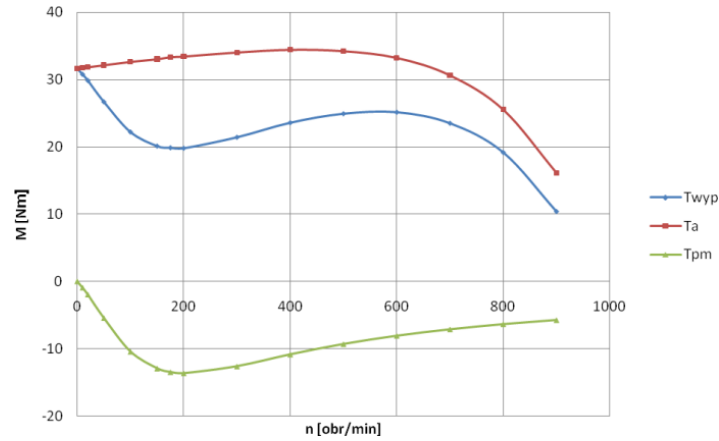
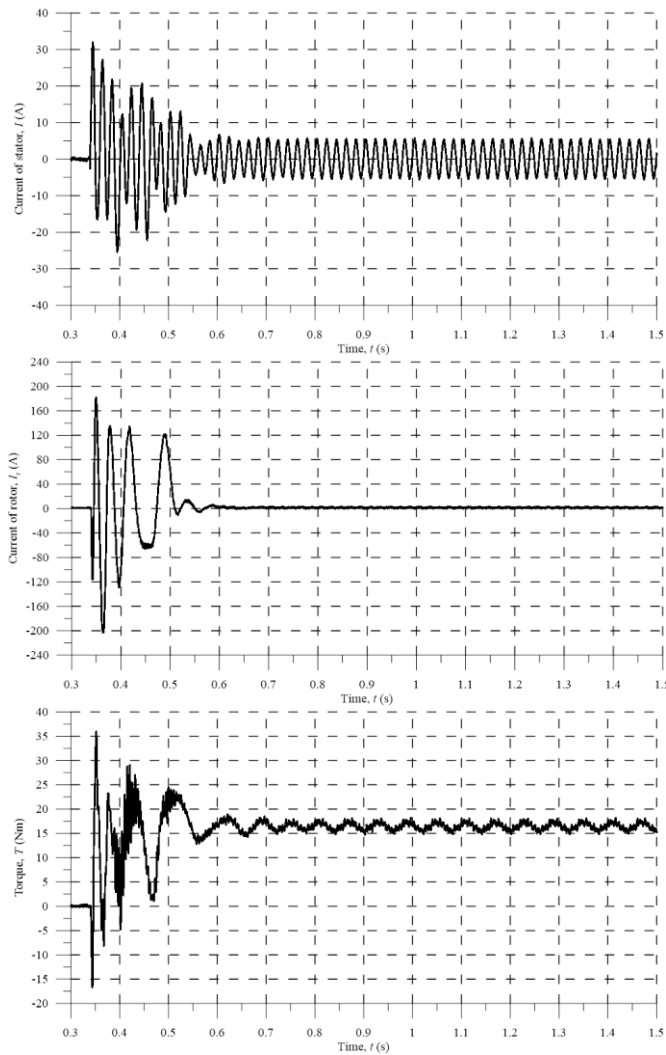


Fig. 5. Calculated average torque characteristics: asynchronous T_a and from magnets T_{PM}

The model motor was subjected to laboratory tests. Fig. 6 shows the recorded waveforms: stator current, rotor current, torque, and rotational speed during start-up. Fig. 7 shows the measured synchronous characteristics: stator current I , power factor $\cos \varphi$, and efficiency η as a function of load torque.



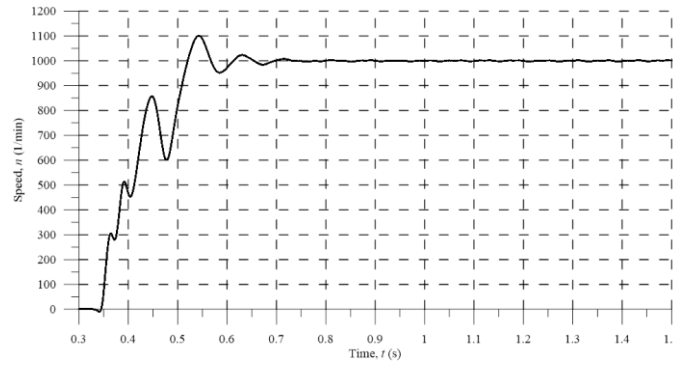


Fig. 6. Recorded waveforms during start-up: stator and rotor currents, load torque, and rotational speed, with shorted slip rings

Asynchronous starting of the model motor, with direct supply from the grid and shorted slip rings, is realized. The waveforms of current, torque, and rotational speed during start-up are disturbed by the synchronous torque excited by the permanent magnets, but their average values are similar to those in a squirrel-cage induction motor.

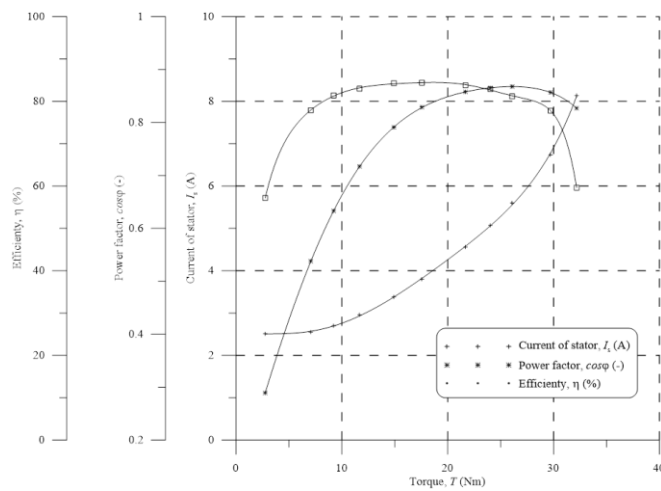


Fig. 7. Measured characteristics: current, power factor, and efficiency as a function of load torque

Tab. 2 presents the rated parameters of the SUDfL-100B slip-ring induction motor and the permanent magnet model motor (Glinka T., Bernatt J., 2017).

Table 2. Parameters of the test motor

Parameter	Motor type SUDf100L-6B	
	Induction	With permanent magnets
U_N	3x400V (50Hz)	3x400V (50Hz)
I_s [A]	4.1	3.59
$\cos \varphi$ [-]	0.79	0.81
P_N [W]	1500	1700
T_n [Nm]	16.66	16.2
n_N [rpm]	860	1000
η [%]	67.1	84

The model motor excited with permanent magnets with asynchronous starting has a sufficiently large starting torque. It self-synchronizes and, after synchronization, operates as a synchronous motor. This type of motor can be used for any electric drive that does not require speed control. If speed control is required, permanent magnet-excited motors can be supplied from inverters, like any induction motor. Compared to an induction motor performing the same task, the permanent magnet-excited synchronous motor has higher energy efficiency and power factor.

Starting the motor with the use of a frequency converter

If several identical machines driven by permanent magnet synchronous motors are installed in a given facility, installing a central starting system for synchronous motors is advantageous, as shown in Fig. 8 (Bernatt, Gawron and Glinka, 2021). This is an alternative to the solution where motors with permanent magnets and a starting winding are used.

The central starting system for permanent magnet excited synchronous motors M consists of an AC-DC-AC inverter 1, a synchronizer 3, and circuit breakers W . All system components are three-phase. Fig. 8 shows one AC-DC-AC inverter 1 and a group of four motors M 2. The inverter 1, synchronizer 3, and each of the motors M 2 are connected by one circuit breaker W to the power grid $U1$ and by another circuit breaker W to the busbars $U2$.

The AC-DC-AC inverter 1 should have a frequency f regulation range from a minimum frequency of, for instance, 3 Hz to 55 Hz. After connection to the inverter, the motor starts with a constant magnetic flux. The AC-DC-AC inverter 1 starts each motor M 2 separately. Synchronizer 3 can be located in the AC-DC-AC inverter 1 and is an integral part of inverter 1. Synchronous motors M , used in drive systems of working machines, are high-power and have a rated voltage of 6 kV or 10 kV. The voltage of the power grid $U1$ from which the motors are supplied is also 6 kV or 10 kV. Inverters for 6 kV or 10 kV are expensive. For starting motors with a rated voltage of 6 kV and 10 kV, using a lower voltage inverter is advantageous, as they are much cheaper. This solution connects the AC-DC-AC inverter 1 to the power grid $U1$ through an inverter transformer 4. The output voltage of inverter 1 supplying the busbars $U2$ should be equal to the rated voltage of the motor M . This is achieved by connecting the output of inverter 1 to the busbars $U2$ through transformer 5, as shown in the figure.

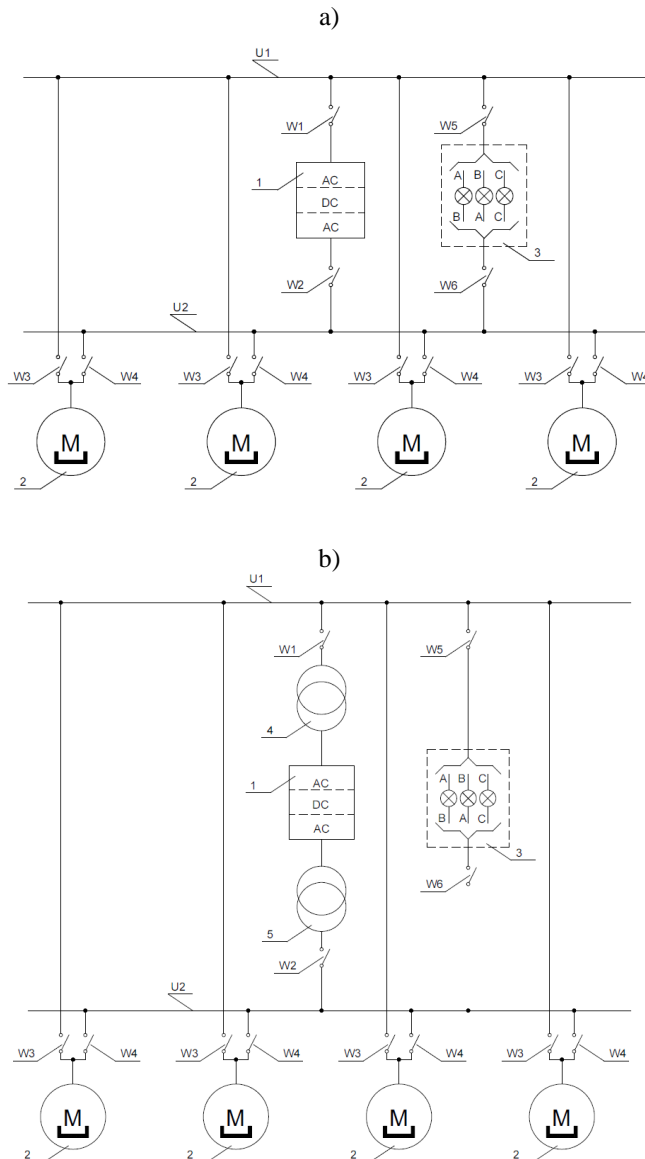


Fig. 8. Connection diagram of the AC-DC-AC inverter, motors M , and synchronizer with the power grid $U1$ and busbars $U2$: a) the inverter is supplied directly from the grid, b) the inverter is supplied through a transformer.

The starting of each motor M 2 proceeds as follows:

- Circuit breaker W1 connects the AC-DC-AC inverter 1 to the power grid *U1*.
- Circuit breaker W2 connects the inverter 1 to the busbars *U2*, and the minimum voltage frequency is set on the inverter 1.
- Circuit breaker W4 connects the selected motor M2 to the busbars *U2*, and inverter 1 increases the voltage frequency to a subsynchronous value, e.g., 49.5 Hz.
- Circuit breakers W5 and W6 connect synchronizer 3 to the grid *U1* and busbars *U2*.
- The motor is synchronized with the power grid *U1* by adjusting the frequency of the inverter 1.
- When the frequency and phase match, circuit breaker W4 is switched off, and circuit breaker W3 is switched on, and this is the end of the start-up.

The inverter and synchronizer system are ready to start the next motor M. If the next motor is not started, inverter 1 should be switched off from the grid *U1* by circuit breaker W1 and from the busbars *U2* by circuit breaker W2. The Synchronizer 3 should also be switched off by circuit breakers W5 and W6 from the grid *U1* and from the busbars *U2*.

The presented starting system and starting method guarantee a smooth, shock-free start-up of permanent magnet-excited synchronous motors. These motors have the highest energy efficiency of all rotating electrical machines, thus allowing for significant energy savings, which is particularly important in energy-intensive processes in underground mining operations.

Zero-emission power unit with PMSM motor

The motor in a zero-emission power unit forms the most important element of the whole power and control system. It is related to its correct selection, which enables an appropriate efficiency increase for the whole power and control system. In power and control systems, due to trends in electric power units, motor efficiency and the possibility of energy recuperation more and more often, the use of a synchronous motor with permanent magnets is foreseen. Values of losses in iron, both in the case of motors with permanent magnets and asynchronous motors powered from a power electronic converter, are similar due to the similar construction of stator sheet packets. In motors with permanent magnets, losses in stator copper windings are, however, smaller as these motors require fewer windings for a phase at the same supply voltage value. However, due to a lack of winding in the rotor and a synchronous operation, losses in the motor rotor with permanent magnets do not occur in practice. The only source of losses in the rotor includes only additional losses. The sum of losses in the motor with permanent magnets is smaller, so its efficiency is higher, which causes its heating to be smaller. Motors with permanent magnets get more and more popular mainly due to:

- a higher efficiency in the whole scope of rotation speed change,
- a big torque overload capacity,
- a wide scope of rotation speed change,
- smaller overall dimensions (compared to induction motors and/or DC motors),
- an efficient control of rotation speed,
- a bigger operational reliability compared to DC motors.

The application of more and more perfect control systems connected with good operational properties of motors with permanent magnets themselves caused DC motors with mechanical commutators and induction motors to be put out of service more and more often.

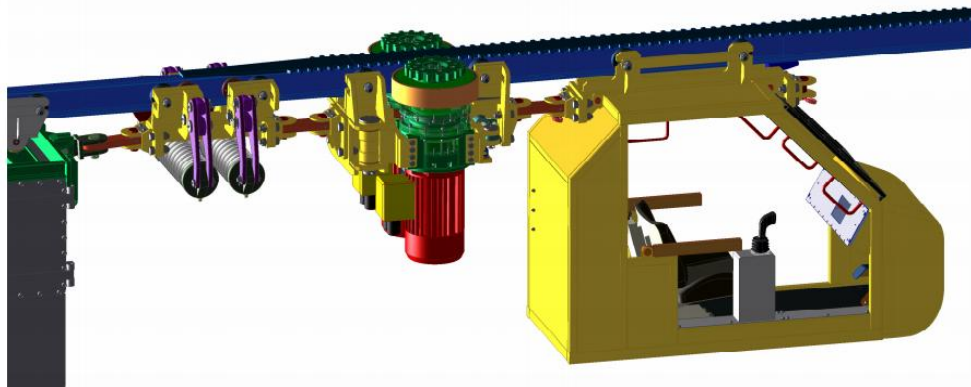


Fig.9. View of a haulage unit part with power unit

Due to permanent magnets, PMSM motors can generate torque at zero speed. For the operation, they usually require an inverter to be controlled digitally. Synchronous motors with a permanent magnet are usually used in high-efficiency and capacity drives. Their characteristic features include a soft rotation motion within the whole scope of the motor rotation speed, full control of torque at zero speed, and fast acceleration and deceleration.

An example of an efficient application of a zero-emission power unit is the suspended GAD-1 battery haulage unit, whose part is shown in Fig. 9 (Mróz et al., 2012; Lutyński, 2021).

A successful condition while implementing the haulage unit with a battery supply was to ensure at least an 8-hour operation without an exchange of a cell battery while keeping the smallest weight of the haulage unit itself. Due to the limited energy density of traditional battery acid cells, the only way to achieve the assumed objective was an application of new generation cells and recuperate energy during transport in an inclined working, in the downhill direction when electric motors work as generators, acting as brakes. The current generated by motors through frequency converters is directed to the battery. Hence, it is necessary to maintain a certain reserve of battery capacity for storing additional energy. Energy balance, which is connected with the transport direction of uphill and downhill loads, is closely related to this problem. Therefore, an estimation of energy balance requires the following data:

- how the transported loads will change their location level from the place of their loading and unloading;
- how big weights will be transported;
- how long the individual sections of the route will be and what inclination they will have;
- what the drive efficiency will be like during the motor action;
- what the energy recuperation, while braking during a generator action, will be like.

Based on this data, it is possible to determine a permissible level of battery charge resulting from:

- an increase or reduction of the potential energy of the load and haulage unit;
- energy losses for overcoming movement resistance on individual route sections, energy losses resulting from the efficiency of mechanical devices;
- energy losses as the result of the efficiency of electrical devices.

Therefore, a situation cannot be excluded that the energy balance during a transport operation will be positive. Such a case can happen when a transport of load on a big inclination is conducted downhill, and its return trip without any load is uphill. For example, suppose a haulage unit with a load of a weight of 25 t covers the level difference of 100 m along the distance of about 500 m from the recuperation braking during a trip with a load downhill. In that case, the recuperation system can deliver about 19 MJ of energy to the battery, but during the return trip of the unloaded haulage unit of 13t weight – about 15 MJ of energy will be used. In this case, a battery exchange will not be needed because the energy balance will be positive, reaching +4 MJ. For a comparison of the amount of energy in the above-mentioned example, the batteries of the GAD-1 haulage unit are capable of storing 570 MJ of energy.

The GAD-1 haulage unit is equipped with four powered trolleys, and each power trolley is equipped with two power assemblies (Fig. 10).

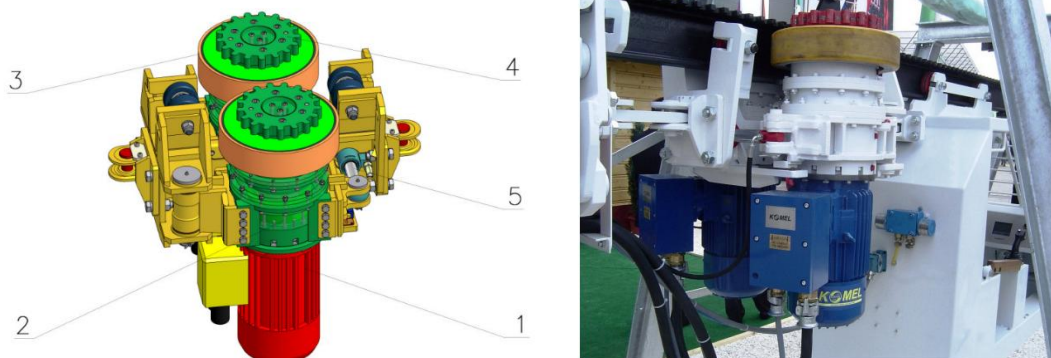


Fig.10. Construction of the power trolley (on the left) and a single power assembly installed in the power trolley (on the right): (1-PMSM motor; 2-gear; 3-friction wheel; 4-sprocket; 5-hydraulic cylinder)

The character of the haulage unit operation forced the application of motors at different speeds in individual powered trolleys, which caused a necessity to supervise a change of the power mode by the control system based on the appropriate algorithm.

The power source of the powered trolleys is an accumulator battery of 250 V DC voltage, consisting of three assemblies of lithium cells of 150 Ah capacity and one – of 200 Ah capacity. Additionally, an induction motor of a hydraulic pump is powered by the 200 Ah assembly. The energy from the assemblies of batteries, through flameproof connectors, is supplied to the power module, in which, with the use of eight inverters, 3-phase voltage of controlled frequency and amplitude powering eight brushless motors with permanent magnets is obtained. The ninth inverter, which has 188 V voltage and 50 Hz frequency, serves to power the hydraulic pump's induction motor. During braking, the motors generate energy, which, through the same converters, goes to the battery assembly. The control system watches over a situation, ensuring that batteries always have a capacity reserve, enabling an energy return from the braking operation.

The parent control system of the haulage unit, acc. to the block diagram (Fig. 11) (Drwięga, Polnik, Kalita, 2015), has a dispersed structure connected in series by the CAN digital bus. It is characterized by a strong resistance to disturbances and high reliability, which is obtained through data transmission in the form of a differential voltage signal and by hardware support for the protocol and error control. Such buses are commonly used in cars. The CANopen communication protocol, whose advantage includes bus unification, will be implemented. It gives the possibility of connecting subassemblies of different producers and enables a connection of an application designed for diagnosing and configuring the CAN bus.

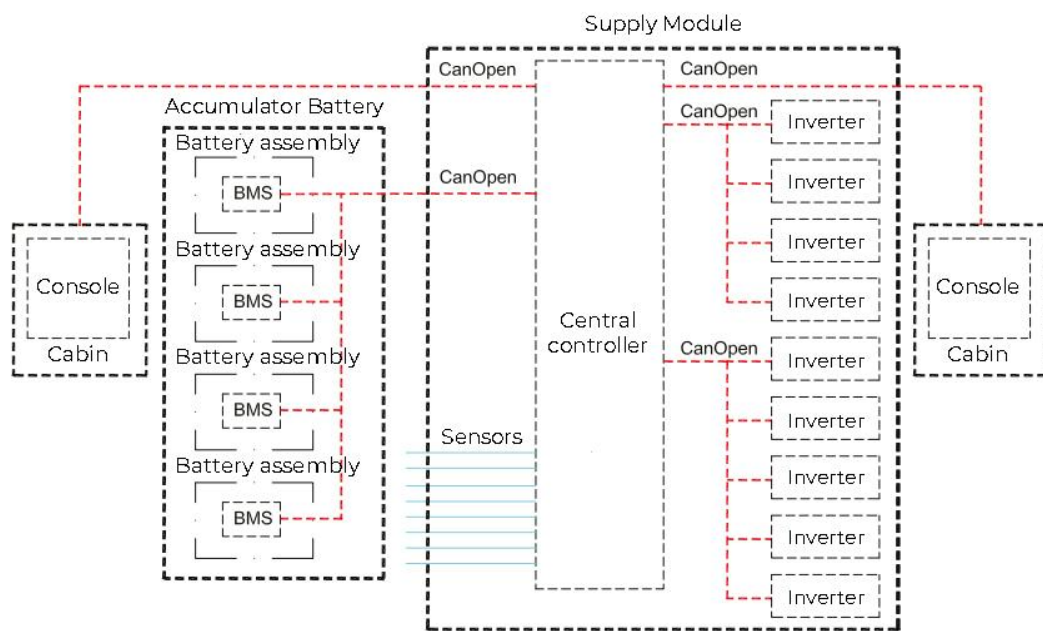


Fig.11. Block diagram of the parent control system

Management of power distribution in different phases of operation (start-up, trip with changeable loading, temporary overloads, braking with energy recuperation) and in the conditions of changeable charging state of battery requires an application of vector control techniques of a multi-motor power system and an appropriate selection of components parameters as well as an elaboration of security algorithms.

Due to an emission-free operation, a low level of released heat and a relatively silent operation, the suggested solution is very competitive in relation to commonly used devices of this type with a diesel drive. As a result of the elimination of exhaust emissions, the work comfort of operators is increased.

References

- Bao Y., Mehmood W., Feng X. (2012). Super premium efficiency linestart permanent magnet synchronous motor: design, test and comparison. Petroleum and Chemical Industry Technical Conference (PCIC)
- Baranski M., Szlag W., Lyskawinski W (2019).. An analysis of a start-up process in LSPMSMs with aluminum and copper rotor bars considering the coupling of electromagnetic and thermal phenomena, Archives of Electrical Engineering, vol. 68, no. 4, pp. 933-946, DOI: 10.24425/aee.2019.130693.
- Bernatt J., Gawron S., Glinka T., Pacholski E. (2017). Staszewski K.:Wirnik silnika elektrycznego z magnesami trwałymi. Patent PL 226639. Instytut Napędów i Maszyn Elektrycznych KOMEL
- Bernatt J., Gawron S., Glinka T. (2021). Silnik synchroniczny wzbudzany magnesami trwałymi z rozruchem asynchronicznym. Patent PL 239127. Sieć Badawcza Łukasiewicz - Górnośląski Instytut Technologiczny

- Bernatt J., Glinka T., Polak A. (2023). Układ rozruchowy silników synchronicznych wzbudanych magnesami trwałymi. Patent PL 243911. Sieć Badawcza Łukasiewicz - Górnośląski Instytut Technologiczny
- Bołoz Ł. (2024) Generating models for numerical strength tests of 3D printed elements. *Management Systems in Production Engineering*. 2024, Volume 32, Issue 3. pp. 372-379. doi: 10.2478/mspe-2024-0035
- Damaki A, Mirsalim M. and Farrokhzad E (2010).: Line-Start Permanent-Magnet Motors: Significant Improvements in Starting Torque Synchronization and Steady-State Performance, *IEEE Transactions on Magnetics*, vol. 46, no. 12, pp. 4066-4072, 2010.
- Drwięga A., Polnik B., Kalita M. (2015). Innowacyjne urządzenia transportowe z elektrycznym napędem akumulatorowym. *Maszyny Górnicze* Nr 3, pp 36-44
- Fei, W.; Luk, P.C.K.; Ma, J.; Shen, J.X.; Yang, G. A. (2009). High- Performance Line-Start Permanent Magnet Synchronous Motor Amended From a Small Industrial Three-Phase Induction Motor. *IEEE Transactions on Magnetics* vol. 45, no. 10, pp. 4724-4727. doi: 10.1109/TMAG.2009.2022179
- Glinka T., Bernatt J. (2017). Asynchronous Slip-Ring Motor Synchronized with Permanent Magnet. *Archives of Electrical Engineering*. Nr 1, pp. 199-206
- Ghoroghchian F., Aliabad A., Amiri E., Poudel B, (2017) Line start permanent magnet synchronous motor with dual magnetic polarity. *IEEE International Electric Machines and Drives Conference (IEMDC)* DOI: 10.1109/IEMDC.2017.8002110
- Gwoździewicz M., Ciurys M. (2023). Line Start Permanent Magnet Synchronous Motor rotor Designing Methodology. *Przegląd Elektrotechniczny* Nr 12, pp 220-227
- Gwoździewicz M, Zawilak J (2013) Single-phase line start permanent magnet synchronous motor. Rotor construction and stator winding optimization. *Archives of Electrical Engineering*, Nr 2, pp. 227-236
- Jedryczka, C.; Wojciechowski, R. M.; Demenko, A. (2014). The influence of squirrel cage geometry on synchronization of line start permanent magnet synchronous motor. 9th IET International Conference on Computation in Electromagnetics (CEM). doi: 10.1049/cp.2014.0235
- Korski W., Horak W., Bołoz Ł., Nistrój R., Kozłowski A. Lightweight lhd bev loader with an individual drive for each wheel. *Management Systems in Production Engineering*. 2023, Volume 31, Issue 3. pp. 281-289. doi: 10.2478/mspe-2023-0031
- Lu Q., Huang X., Ye Y., Fang Y. (2012). Experiment and analysis of high power line start PM motor. *Przegląd Elektrotechniczny* Nr 2
- Lutyński A. (2021). KOMAG activities in the domestic and international research areas. *Mining Machines* Vol. 39 Issue 4, pp. 47-60
- Mróz J., Skupień K., Drwięga A., Budzyński Z., Polnik B., Czerniak D., Dukalski P., Brymora L. (2012). Akumulatorowy ciągnik podwieszany GAD-1 z innowacyjnym napędem, jako alternatywa rozwiązań z napędem spalinowym. *Maszyny Elektryczne* Nr 3 (96), pp 83-90
- Ugale, R. T.; Chaudhari, B. N. Rotor Configurations for Improved Starting and Synchronous Performance of Line Start Permanent-Magnet Synchronous (2017) Motor. *IEEE Transactions on Industrial Electronics*, vol. 64, no. 1, 138-148, doi: 10.1109/TIE.2016.2606587
- Zawilak T., Zawilak J. (2014). Patent PL 218489. Wirnik silnika synchronicznego z magnesami trwałymi. Politechnika Wroclawska
- Zawilak T., Zawilak J. (2016). Silnik synchroniczny wzbudzany magnesami trwałymi w napędzie młyna kulowego. *Maszyny Elektryczne – Zeszyty Problemowe* Nr 3, pp. 169 -173
- Zawilak T. (2013). Utilizing the deep bar effect in direct on startof permanent magnet machines. *Przegląd Elektrotechniczny* No 2, pp. 177 – 179
- Zhou, Y.; Huang, K.; Sun, P.; Dong, R. Analytical Calculation of Performance of Line-Start Permanent-Magnet Synchronous Motors Based on Multidamping-Circuit Model. *IEEE Transactions on Power Electronics* 2021, vol. 36, no. 4, 4410-4419, doi: 10.1109/TPEL.2020.3025172